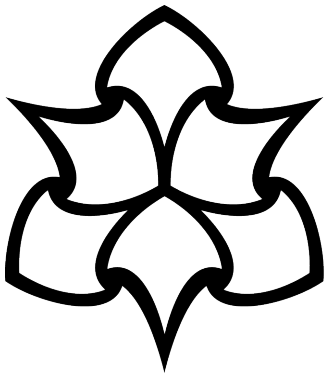

Published in Ecological Indicators – Accepted 7 Oct 2020 – DOI https://doi.org/10.1016/j.ecolind.2020.107058

Mapping regulating ecosystem service deprivation in urban areas: a transferable high-spatial resolution uncertainty aware approach

Authors: Fraser Baker*, Graham R. Smith, Professor Stuart J. Marsden and Dr Gina Cavan

During processing of this manuscript all authors were affiliated to:

Ecology & Environment Research Centre, Department of Natural Sciences, John Dalton Building, Manchester Metropolitan University, Chester Street, Manchester, M1 5GD, UK

** Corresponding author:*

Email: f.baker@mmu.ac.uk

Highlights

1. Maps of ecosystem services to demand at scale (100m) of micro-scale benefit transfer
2. Coldspot concept investigated to identify neighbourhood ecosystem deprivation
3. Novel sensitivity analysis evidencing spatial landcover dependency in map uncertainty
4. Demand measures evidenced as important to control spatial prioritisation measures
5. Map uncertainty countered by overlapping outputs from different parameter settings

Abstract

Maps of regulating urban ecosystem services (UES) aid identification of priority areas for green-blue infrastructure investment to improve urban resilience to environmental hazards. Current mapping approaches, however may present coarse spatial resolutions and often fail to consider how UES flows serve resident demand at the appropriate micro-scale. In addition, prohibitive costs involved in collecting primary data to validate UES model parameters to local conditions may enforce the use of proxy methods, thereby inferring ambiguity in parameterisation and thus uncertainty in mapping outputs. This study examines both issues through the implementation of a novel high-spatial resolution approach to map multiple urban regulating ecosystem service (temperature regulation, stormwater absorption, and carbon storage) deprivation in Manchester, UK. Poorly performing UES areas are defined as the lowest 10% combined ecosystem service indicator values ('coldspots') at 100m grid resolution. Coldspots are compared to population demand levels, disaggregated from weighted population estimates, indicating neighbourhoods deprived of UES. Uncertainty in proxy method implementation is examined using combinations of uncertain UES parameter settings (*n* = *16*) within various demand measures (*n* = *3*) to measure changes in relationships between UES, and variation in final mapping outputs across the study area. Uncertainty is therefore quantified as an interactive process, whereby input parameter uncertainty affects local uncertainty in map outputs, due to the varying composition in associated landcover. As explicit sensitivity analysis in current UES mapping studies is limited, the study demonstrates how ambiguity in method parameterisation may impact both current and future UES map exercises. Complex interactions governing spatial variance in map uncertainty may therefore be addressed through identification of consistent areas of interest

Abbreviations in this manuscript: UES = Urban regulating ecosystem services; UGBI = Urban green-blue infrastructure; SCS-CN = Soil conservation society curve number method; CN = Curve Number

(e.g. hot-spots, coldspots) by contrasting outputs realised from different parameterisations. As such, the study demonstrates the mapping approach as a novel transferable city-wide visualisation tool, using accessible data and methods, to investigate regulating UES deprivation at practical scales of green-blue investment required to retrofit existing urban infrastructure.

Keywords: regulating ecosystem services; mapping; deprivation; urban; environmental risk; uncertainty analysis

1. Introduction

Regulating urban ecosystem services (UES) of urban green-blue infrastructure (UGBI) benefit urban residents by moderating environmental hazards associated with urbanization (Gomez-Baggethun et al. 2013). As climate change is projected to increase the frequency and severity of extreme weather conditions, the localised provision of regulating ecosystem services such as urban cooling, atmospheric carbon storage, and stormwater absorption, will become increasingly important to safeguard human health and well-being (Kabisch et al. 2016). The spatial mapping of multiple regulating UES is therefore useful to identify neighbourhoods where strategic UGBI interventions may benefit local resident well-being (Kabisch et al. 2016, Pulighe et al. 2016). However, despite increased access to high-spatial resolution geospatial data in recent years, that has enabled improvements in UES mapping methods, the practical influence of resulting information products within urban planning concerns appears limited (Haase et al. 2014, Woodruff & BenDor 2016). Improvements in the effective spatial communication of UES benefits are arguably required to support the conservation and enhancement of local UGBI resources.

A primary challenge for UES analyses is the appropriate spatial representation to represent real world UES processes. UES measures amalgamated within census tracts, administrative boundaries or land-use/land-cover areas, are beneficial for comparing a wide range UES benefits (e.g. economic, social and cultural) to either local demand for such services, such as in neighbourhoods containing high-need demographic groups, or within areas of local planning concern (Baró et al. 2017, Cabral et al. 2016, Kroll et al. 2012). However, as specific regulating UES benefits may occur at the micro-scale (e.g. particulate capture by individual trees, or localised air cooling) alternative spatial representations may better represent micro-scale variation in benefit flows to local residents (Andrew et al. 2015). For example, an administrative area may consist of a distinct residential urbanised area with minimal UGBI cover, adjacent to a large park consisting primarily of

UGBI. Due to morphological constraints, the temperature regulation benefits provided by the parkland may have limited impact within the residential area (Coseo & Larsen 2014). However, in this instance the significant presence of the parkland UGBI results in overestimation of temperature regulation benefits when calculating a single service value for the area as a whole (Gomez-Baggethun et al. 2013). In contrast, UES represented within grid structures provide more appropriate measures of spatial variation in continuous regulating UES environmental processes across heterogeneous urban environments (Holt et al. 2015, Kremer et al. 2016a, Langemeyer et al. 2020). Studies demonstrate the benefits of service demand indicators at fine scale resolution to map overall UES values (Baró et al. 2016, Larondelle & Lauf 2016), but remain limited in number, and may rely on data relevant to the specific study area. To improve applicability of UES mapping approaches, further investigation of adaptable grid based UES benefit to demand indicators across different urban areas are thus required.

In addition, current mapping outputs may implicate an unquantified level of uncertainty, through the combination of various methods and assumptions required to assess bundles of UES. Whilst models validated with primary data that represent local ecological and environmental conditions are preferred, the costs to collect and process such data for particular UES may prove prohibitive for whole city areas (Schröter et al. 2015). In comparison, proxy methods provide a time and cost-effective alternative but may result in spurious map outputs due to the direct transfer of findings to inappropriate ecological representations (Eigenbrod et al. 2010). Studies may counter this issue through approaches tailored to the local urban environment and associated data. However, as quality of input data may vary considerably between study areas, such mapping approaches may have limited application in other urban areas (Haase et al. 2014). Due in part to a current lack of standardisation in methods, UES knowledge transfer between urban areas is limited (Kremer et al. 2016b). UES mapping approaches applicable to different urban environments thus require

understanding of how input data of varying quality may cause ambiguity in the parameterisation of component methods, and thus influence final map products (Schulp et al. 2014). Whilst consideration of mapping uncertainty is often discussed in UES studies, it is rarely investigated in quantified terms (Andrew et al. 2015, Zhao & Sander 2018).

In order to advance current methods for mapping UES, this study aims to address the aforementioned issues by transforming current UES mapping methods into an accessible high-spatial resolution regulating UES approach. A case study implementation of the mapping approach for Manchester, UK, demonstrates the benefits of the methods applied. Results from this exercise provide recommendations for application of the approach in other urban areas, in addition to generating knowledge for wider UES mapping research.

2. Methods

2.1 Study Area

Manchester is a post-industrial city located in the North-west region of England, UK (***Figure 1***) covering an approximate area of 115 km^2 (UKDS 2017), with an estimated 2016 population of 541,000 (4,716 people/km^2) (MCC 2018). Currently, UGBI covers approximately 49% of the total city area, with significant UGBI contained within parklands and other natural resource areas (Dennis et al. 2018). In addition, UGBI varies according to residential housing characteristics, with pre-1919 (46.2% of housing stock; typically terraced housing), and post-1919 residential areas estimated to contain on average 11.8% and 37.8% tree cover respectively (Hall et al. 2012). Due to heterogeneity in local UGBI resources, residents in the city experience varying regulating UES (Gill et al. 2007); therefore, the city provides a useful case study area to develop a regulating UES mapping approach.

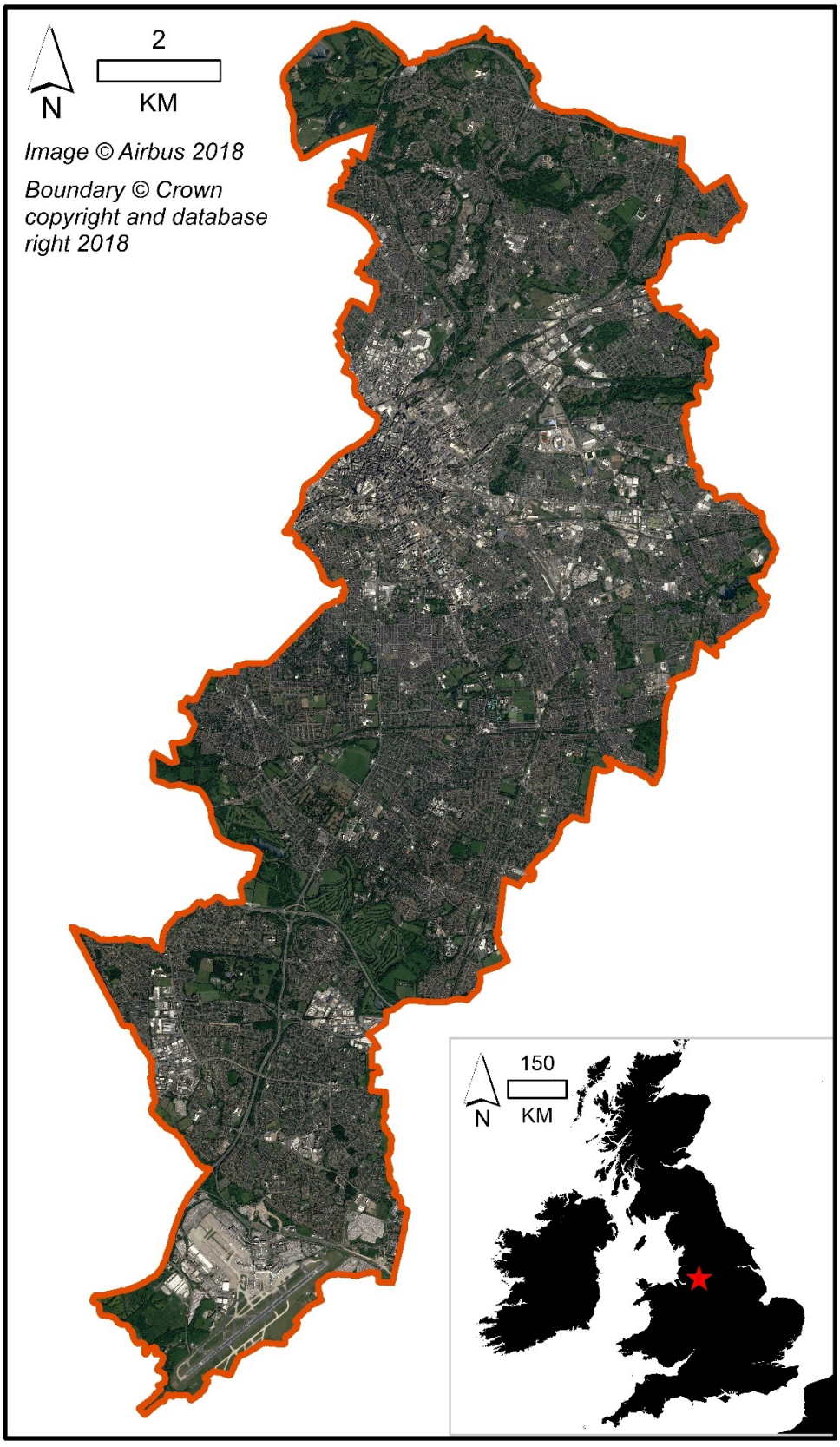
N
2
KM
Image © Airbus 2018
Boundary © Crown copyright and database right 2018
N
150
KM

Figure 1 – Location of Manchester within UK

2.2 Overview of mapping approach

Environmental hazards affecting study area residents include pluvial and fluvial flooding and heat stress from extreme temperatures, in addition to larger scale environmental risks posed by global warming (Carter et al. 2015). Therefore, regulating services chosen for the mapping approach include temperature regulation, carbon storage, and stormwater absorption, due to benefits in regulating urban environmental risks for current and future climate conditions (Carter et al. 2015). Models for UES indicators that are feasible for micro-scale citywide analysis were chosen following a review of UES mapping literature (**Table 1**). The approach uses a regular grid cell structure (100m resolution) to provide a measure of UES indicators in relation to UGBI change across the continuous urban environment (Holt et al. 2015). Within this approach, disaggregated census population estimates represent levels of resident demand for local regulating UES (Baró et al. 2017).

Table 1 – Methods and indicators chosen for UES

UES	*Description of service*	*Chosen method**	*Modelled indicator measure*	*Study area validation***
Temperature regulation	Reduction of localised temperatures during hot weather conditions	Geographically weighted regression models to estimate the influence of local UGBI on remotely sensed	Predicted LST (max LST = 0 service value; min LST = 100% service value)	YES

		Land Surface Temperature (LST; °c).		
Carbon storage	Storage of carbon within vegetation biomass	Transfer of carbon storage values per Land-use Land-cover categories in UK based carbon storage studies to Land-cover categories within the case study.	Predicted C kg m^2 (max C kg m^2 = 100% service value; min C kg m^2 = 0% service value)	NO
Stormwater absorption	Reduction of runoff and local flooding pressures through capture of precipitation by UGBI	SCS-CN (USDA 1986) method to estimate runoff reduction potential (CN) of localised UGBI resources.	Quantified CN (Max CN = 0% service value; Min CN = 100% service value)	NO

* *Further description of methods provided within the following sections; ** Model estimates validated to independent measures of environmental conditions within the study area.*

Due to the excessive costs of acquiring independent reference data, parameters for carbon storage and stormwater absorption models (**Table 1**), in addition to demand disaggregation methods, are not validated to study area conditions, and therefore infer a degree of uncertainty. Following a

pragmatic interpretation of the mapping approach, sensitivity analysis was investigated how uncertainty in proxy method assumptions may potentially impact UES map outputs in further mapping applications. The influence of proxy method choice upon relationships between unique UES, and combined UES indicators, in addition to mapping combined UES deprivation ('Coldspots') was therefore investigated using (n = 16) service model parameter settings within various (n = *3*) demand measures (Eigenbrod et al. 2010). Combined UES deprivation (*Coldspot*) areas identified through overlap of deprivation areas for each parameter setting, aim to reduce potential mapping uncertainty and thus demonstrate the overall benefits of the mapping approach. **Figure 2** presents the case study workflow, with methods described in the following sections.

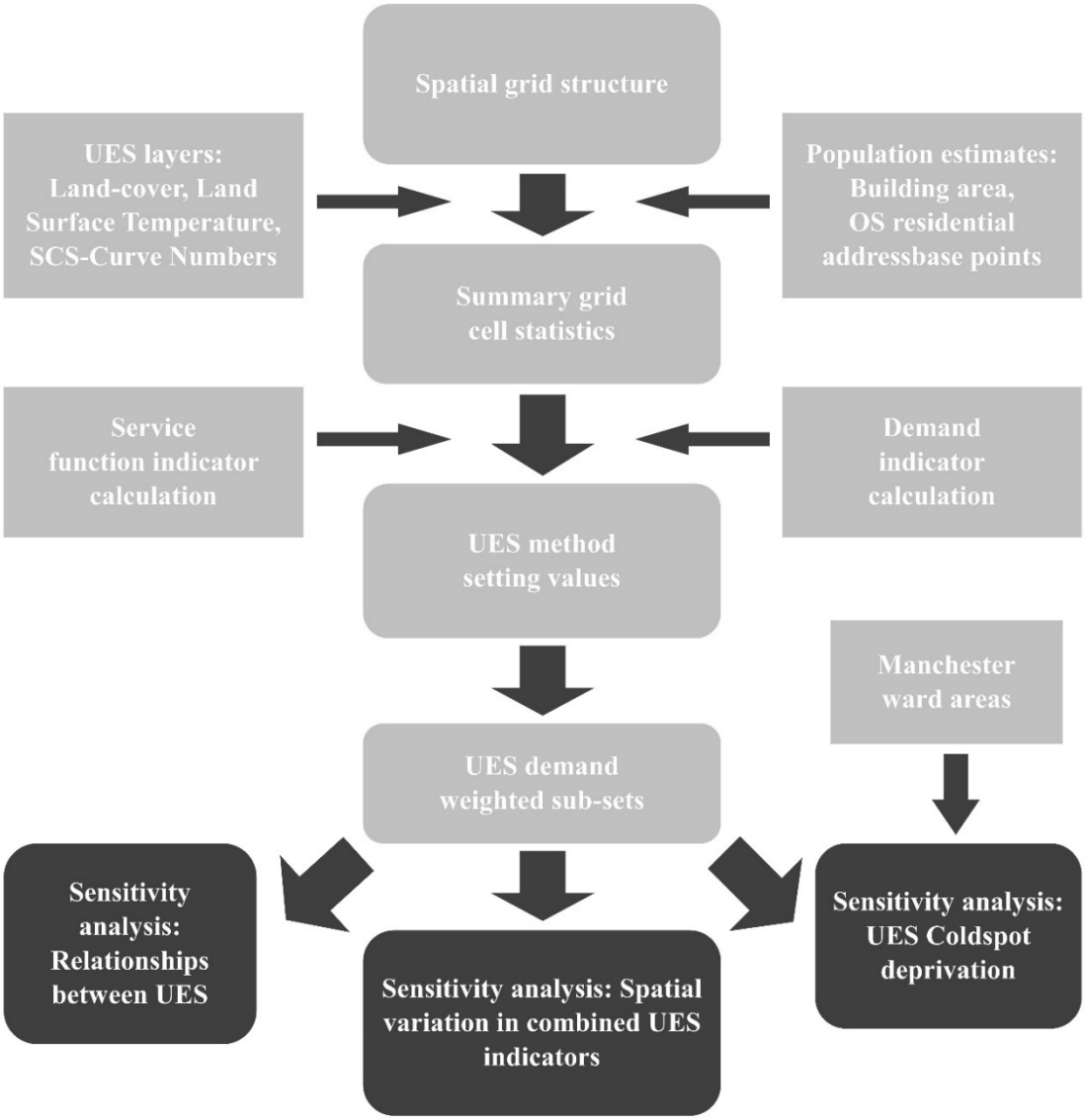

Figure 2 **-** Case study workflow

2.3 Urban landcover

An urban landcover map representing five classes (buildings, non-vegetation (artificial and bare Earth surfaces), tree Canopy, non-tree vegetation & water) was generated to provide geo-referenced ecological map data to estimate UES values (see ***Table 2*** and ***Figure 3***). The data was

scaled at 2m pixel resolution (now widely available) to generate land-cover products available in similar UES mapping studies (see Derkzen et al. 2015, Kremer et al. 2016a).

Table 2 – Data, methods and class descriptions used to generate the urban landcover map

Process	Reference data	Methods	Classes from methods*
1	Mastermap topography layer (May 2017 version; Edina Digimap 2017)	Land parcel and surface feature extents represented as polygon areas; attribute data used to categorise initial class area where possible	All classes
2	Tree audit data (CityOfTrees 2011)	Represents canopy extents (> 1.5m) of trees and woodland; provides masking feature to re-classify all landcover classes as trees	Tree canopy
3	True-colour aerial imagery (12.5cm resolution; collected June 2009 – 2015; Getmapping 2017)	Classified into a vegetation mask using a threshold with image band data; used to assign non-classified pixels as either non-tree vegetation or non-vegetation appropriate	Non-tree vegetation; Non-vegetation

* Buildings = permanent building structures; Non-vegetation = Artificial and Bare Earth; Water = Water bodies and channels; Tree Canopy = tree canopy extents; Non-tree vegetation – vegetation not considered as trees, such as shrubs and grasses.

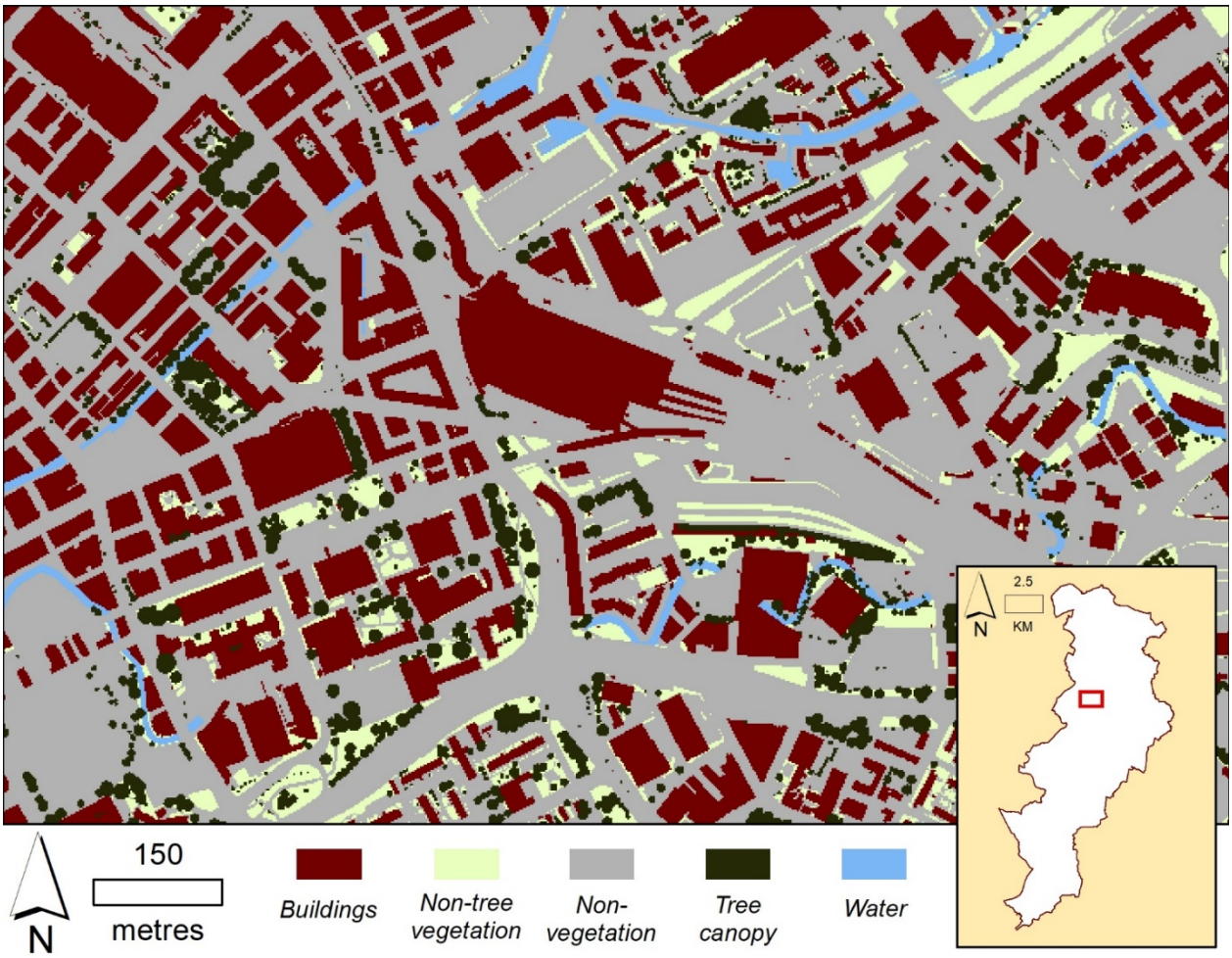

Figure 3 – Example of mapped urban land cover for central Manchester

2.4 Temperature regulation

Land surface temperature (LST) represents the temperature of ground surface layers and is a governing indicator of thermal energy transfer for above ground ambient air warming (Oke 1988), with excessive LST empirically associated with negative health outcomes (Harlan et al. 2014, Laaidi et al. 2011). In comparison to measured ambient air temperatures, which may require significant expense in implementing citywide in-situ monitoring networks (Muller et al. 2013), remotely sensed

LST data is available for entire urban areas, enabling statistical models for temperature regulation indicators. A LST surface was generated using the mono-window method (Wang et al. 2015) using cloud-free imagery (17 July 2017; 30m resolution) from the Landsat-8 Operational Land Imager sensor (USGS 2017). Daytime conditions were warm, with a maximum temperature of 23°C (average 16°C) recorded at the nearby Manchester International Airport weather station (Weather Underground 2017). As spatial patterns of LST in relation to the urban morphology are expected to remain relatively consistent for warmer climate conditions (Oke 1988) the LST surface generated was considered a reasonable representation of excessive heatwave conditions. Geographically weighted regression was implemented (in ArcMap version 10.3 by ESRI) using ordinary least squares regression (equation 1) to statistically infer the causal relationship of UGBI (proportion of UGBI per cell = pUGBI) upon LST as it varies according to localised change in urban morphology. Predicted mean LST per cell (pLST) provided the measure for estimating temperature regulating indicators.

$$pLST_{CELL} = a + b \cdot pUGBI_{CELL} \quad [1]$$

2.5 Carbon storage

Due to the prohibitive cost of collecting primary data to estimate biomass of local UGBI resources (e.g. vegetation matter and tree characteristics for allometric models) (Derkzen et al. 2015, Holt et al. 2015) above-ground carbon storage was calculated based upon findings in UK-based empirical carbon storage studies (See ***Table 3***). Descriptions of carbon storage landcover/land-use categories were matched to case study landcover classes to calculate above ground carbon storage per square metre (C kg m^{-1}) for the associated landcover area. Due to realistic difficulties in interpreting some landcover classes to landcover/land-use descriptions in empirical study, four

different parameter settings were devised to examine the impact on final UES values (***Table 3***). The UES indicator measure is the total carbon stored per cell.

Table 3 – Carbon storage values for four parameter settings

Setting	Land-cover class	Carbon Storage categorisation	Carbon Storage (kg C m^{-2})	Justification for Carbon Density Method
1[A]	Non-Tree	Herbaceous Vegetation	0.15	Herbaceous vegetation only; Non-tree assumed to represent short grasses
	Tree Canopy	Tree	28.46	Assumed to represent tall trees (> 5m height)
2[A]	Non-Tree	Mean: Herbaceous Vegetation, Shrub	5.19	Assumed to represent a mixture of grasses and low shrubs
	Tree Canopy	Mean: Tree, Tall Shrub	21.33	Assumed to represent a mixture of tall shrubs and trees
3[B]	Non-Tree	Sport and Leisure	0.68	Sports and leisure land use assumed to represent a mixture of vegetation types

	Tree Canopy	Mixed forest	3.28	Mixed forest only
4[B]	Non-Tree	Green Urban Areas	0.09	Green urban areas only (grassy areas)
	Tree Canopy	Broad-leaf Forest	3.80	Broadleaf forest only

[A] category values obtained from Davies et al. (2011) – study provides a quantified survey and extrapolation analysis of carbon storage according to vegetation categories in Leicester, UK; [B] category values obtained from Cruickshank et al. (1998) - study provides a national inventory of carbon storage per land-cover land-use classes in Northern Ireland based upon field-based studies.

2.6 Stormwater absorption

Combined overland-underground catchment scale models enable estimation of stormwater absorption rates of UGBI types through validation of modelled catchment outputs to measured channel outflows (Salvadore et al. 2015). Such methods are computationally expensive for urban districts overlapped by numerous catchment areas, requiring significant data and expertise to implement the required models. In comparison, the Soil Conservation Society curve number (SCS-CN) method (USDA 1986) is a pragmatic alternative widely used in other UES mapping studies (Gill et al. 2007, Kremer et al. 2016a, Tratalos et al. 2007). SCS-CN works as a one-dimensional numerical model that computes the amount of rainfall converted to surface runoff for a given surface area (represented by curve number values) during a rainfall event (USDA 1986). However, unless

independently validated, SCS-CN is a proxy model with curve number values assigned directly between SCS-CN and mapped landcover categories. In the same manner as carbon storage, parameter uncertainty may occur through the interpretation process (see *Section 2.7*) for some landcover classes, therefore four stormwater absorption parameter settings were used to investigate this issue (***Table 4***). Curve numbers (CN) for landcover pixels were assigned by integrating landcover data and underlying soil type (Cranfield University 2018), with stormwater absorption indicators calculated from the areal curve number average per analysis cell.

Table 4 – Curve Number values according to soil groups and chosen Soil Conservation Society (SCS) landcovers per parameter setting

Study area Landcover	Parameter settings	SCS Landcover	Curve Number (CN) per Hydrological Soil Type		
			B	C	D
BUILDINGS	1, 2, 3, 4	Paved, roofs, etc.	98	98	98
NON-VEGETATION	1, 3	Paved, roofs, etc.[1]	98	98	98
	2, 4	Streets and Roads: Paved; open ditches[2]	89	92	93
NON-TREE VEGETATION	1, 2	Pasture: good condition[3]	61	74	80

	3, 4	Brush: good cover[4]	48	65	73
TREE CANOPY	1, 2, 3, 4	Wood: good cover	55	70	77
WATER	1, 2, 3, 4	Water	25	25	25

1 - *Wholly impervious surfaces i.e. Roofs, Asphalt and concrete roads; 2 – Wholly impervious and pervious non-natural surfaces; 3 - Grassland not protected from grazing such as mown grass typical of lawns, playing fields etc. and rough grassland; 4 - Low-standing vegetation such as bushes, weeds and grass*

2.7 Regulating Ecosystem Service demand

Methods for population disaggregation vary depending upon available resources (Stevens et al. 2015, Zandbergen & Ignizio 2010) therefore two disaggregation methods were used to assess choice of method upon final UES mapping outputs. The first method involves areal upscaling of population estimates within census areas to the areal extents of human habitation represented by building footprint area (termed BLD_{POP} here) (O'Brien & Cheshire 2016). This method is financially cost-effective as building footprint areas from the OS are accessible for research in the UK (Edina digimap 2017). However, as no distinction is made between building type (e.g. residential, commercial-industrial), population density is extrapolated across non-residential building areas (Jia et al. 2014, O'Brien & Cheshire 2016). In contrast, the RES_{POP} method uses residential address points from the OS AddressBase Plus product (OS 2018) to weight population towards residential housing (Bhaduri et al. 2007, Zandbergen 2011). However, this method is less accessible due to costs of the associated data. Using both methods, annual population estimates (current estimates available for 2016) for the UK at the Lower Super Output Area (LSOA) level (UKDS 2017) were

disaggregated to generate the relative demand indicators (see *Appendix 1* for population disaggregation workflows).

2.8 Sensitivity analysis – UES relationships and deprivation

Three methods were used to examine the effect of parameter uncertainty upon UES mapping outputs. First, correlation analysis estimates how chosen service parameters and demand methods interact to alter relationships between individual UES (Holt et al. 2015). UES indicator scores were calculated for all parameter settings (*n* = 16; 1 Temperature regulation x 4 Carbon storage x 4 Stormwater absorption settings) within No demand (all cells), BLD_{POP} and RES_{POP} cells. This analysis considered how the mapping approach may perform under differing data assumptions, and also assesses the impact of parameter uncertainty upon UES indicators for models commonly employed in other UES mapping studies.

Second, a manual parameter combination comparison approach investigated the degree parameter uncertainty influences spatial variation in combined UES indicators, defined as percentiles of summed ranks for individual UES (see **Table 1**). Assuming a uniform probability distribution function (PDF) for each uncertain parameter, *n* = 9 unique parameter values were calculated from equal intervals within permitted input parameter range (see **Table 5**). Parameter values were thus altered one by one, in pairs, triples and all parameters together considering all possible parameter interactions for each combination. Mid parameter range values represented the default position for non-altered parameters where applicable. Combined UES indicators per cell were calculated for all parameter interactions, with the range in combined cell UES indicator values defining the level of variation, or uncertainty per parameter combination. This 'brute-force' method was undertaken over a simulation based global sensitivity approach for example, as combined UES indicators require

individual UES indicators for all cells calculated from a uniform set of parameter inputs (Lilburne & Tarantola 2009). This analysis enabled consideration of a) spatial variation in uncertainty across all cells in the study area, b) whether uncertainty increases due to different orders of uncertain parameters, and c) considered the influence of relative magnitudes in parameter uncertainty upon potential mapping outputs.

Table 5 – Probability distribution functions for uncertain parameters

Uncertain carbon storage parameter (kg C m^2)	Key*	PDF parameter range values (Minimum | Maximum | Default)		
Non-tree vegetation	**A**	0.09 | 5.19 | 2.64		
Tree canopy	**B**	3.28 | 28.46 | 15.87		
Uncertain stormwater absorption parameter (CN)		Soil type		
		B	*C*	*D*
Non-vegetation	**C**	89 | 98 | 93.5	92 | 98 | 95	93 | 98 | 95.5
Non-tree vegetation	**D**	48 | 61 | 54.5	65 | 74 | 69.5	73 | 80 | 76.5

* - Identifier for input parameter within parameter combinations; varied parameters notated within brackets e.g. {A, B} represents combined interaction between parameters A and B

Finally, a method to counter potential uncertainty in outputs was assessed by comparing identified 'coldspot' areas at both the neighbourhood (grid cell) and administrative district resolution, to simulate an urban planning exercise to map environmental deprivation at various spatial scales. Coldspots are defined in this study as the lowest 10% of cells using combined UES indicators, and therefore reverse the hotspot concept described in other bundle ecosystem service studies (Anderson et al. 2009, Schulp et al. 2014). Coldspots are then amalgamated to identify the 20% most UES deprived administrative ward areas (Holt et al. 2015) according to the ratio of Coldspot to demand area. Wards were used in this instance, as socio-economic statistics produced at the administrative level therefore enable comparison of relative deprivation levels at the scope of local governance (Baró et al. 2017). As per correlation analysis, this was conducted for all parameter settings across all demand cell weightings.

3. Results

Geographically weighted regression resulted in a model with R^2 = 0.65 and *AIC* = 42952, comparing favourably to the ordinary least squares model (R^2 = 0.45 and *AIC* = 47871). GWR defined temperature regulation indicators therefore remain strongly associated with pUGBI (r = 0.88, p < 0.001), and are therefore positively associated with UGBI benefits for other services. Uncertainty in proxy UES model parameterisation therefore alters these relationships in varying magnitudes according to the relative demand weighting method (**Figures 4 & 5).** Mapped indicators for all UES parameter settings and demand methods are provided in *Appendix 2.*

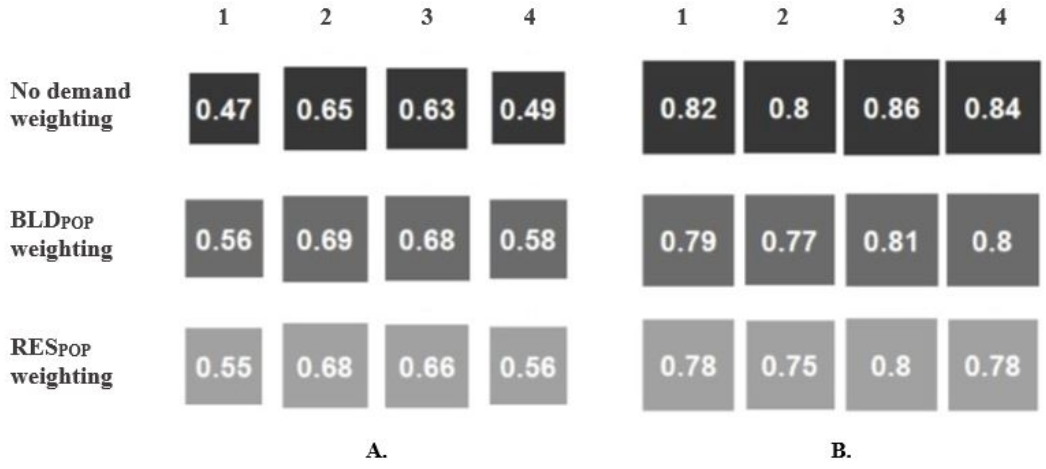

Figure 4 – Correlation (*r*) values between temperature regulation indicators to carbon storage (**A.**) and stormwater absorption (**B.**) indicators for all parameter settings and all demand weighting methods. All *r* values significant at $p < 0.001$ level.

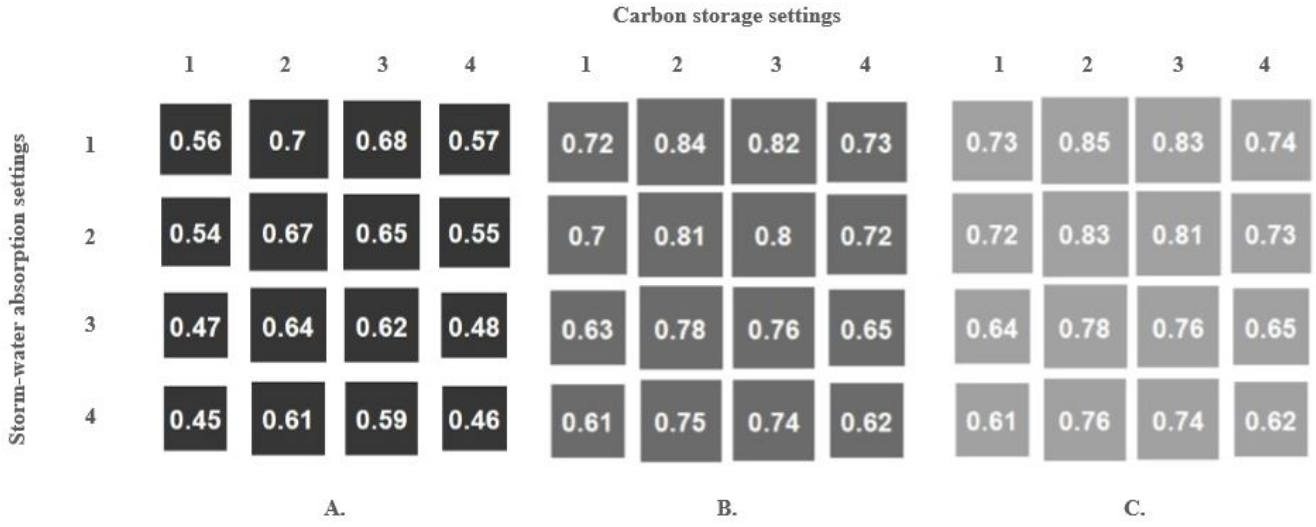

Figure 5 – Correlation values (*r*) between Carbon storage and Stormwater absorption indicators between all parameter settings for No demand (**A.**), BLD_{POP} (**B.**) and RES_{POP} (**C.**) weighted cells. All *r* values significant at $p < 0.001$ level.

Correlation values between temperature regulation and carbon storage indicators increases from no demand cells (mean $r = 0.56$), to the disaggregation methods (mean $r = 0.63$ and 0.61 for BLD_{POP} and RES_{POP} respectively). This trend is however reversed for correlations between temperature regulation and stormwater absorption indicators, with stronger correlation values for no demand cells (mean $r = 0.83$) in comparison to demand weighted cells (mean $r = 0.79$ and 0.78 for BLD_{POP} and RES_{POP} cells respectively). Weighting demand towards building and residential areas in effect removes cells largely covered by water (e.g. cells within reservoirs, water channels) with maximum water coverage per cell varying from 100% for no demand cells, to just 69% and 42.7% for BLD_{POP} and RES_{POP} cells respectively. As water is beneficial for stormwater absorption and temperature regulation services but has no estimated carbon storage benefits (see **Table 5**), the removal of such cells alters relationships between individual UES.

Whilst patterns in relative correlation values between settings remain stable, irrespective of demand method (**Figure 4 & 5**), ranges in correlation values (**Table 6**) vary between demand weighted cells with different landcover proportions. For example, no demand-weighted cells provide the largest range in correlation values and the highest mean UGBI cover (46.4%), contrasting with BLD_{POP} cells, with lowest UGBI coverage (37.4%), and range in correlation values. Correlation differences are small but indicate that variation in relationships between individual UES is constrained somewhat by spatial variation in cell landcover proportions. UGBI proportions per cell are therefore influential, due to the direct association between UGBI landcovers and the majority of uncertain parameters.

Table 6 – Summary statistics for correlations between UES

Demand cells	Temp. regulation to Carbon storage		Temp. regulation to Stormwater absorption		Carbon storage to Stormwater absorption	
	Mean (r)	*Max.(r) – Min.(r)*	*Mean (r)*	*Max.(r) – Min.(r)*	*Mean (r)*	*Max.(r) – Min.(r)*
No demand	0.56	0.18	0.83	0.06	0.58	0.25
BLD_{POP}	0.63	0.13	0.79	0.04	0.73	0.23
RES_{POP}	0.61	0.13	0.78	0.05	0.74	0.24

For combined UES indicators, uncertainty (range in combined UES indicators per cell) generally increases according to the number of interactions between uncertain parameters (**Figure 6**) which influence uncertainty individually by varying magnitudes. As evident, median and maximum combined UES indicator range values for single parameter combinations ({A}, {B}, {C}, {D}) are considerably lower than interacting variations between all parameters ({A,B,C,D}). However, this is not a consistent pattern when travelling from lower to higher order combinations. For example within No Demand cells, parameter variation in tree canopy carbon storage ({B}) values result in more uncertain outputs than parameter combinations {A,C}, {A,D} and {C,D}. The relative importance of single uncertain parameters therefore varies (1^{st} = {B}, 2^{nd} = {A}, 3^{rd} = {D}, 4^{th} = {C}), with carbon storage parameters B and then A interacting to produce greater uncertainty for 2^{nd} and 3^{rd} order parameter combinations. This relationship is associated with the ratio of PDF parameter values against the total range (between no service to maximum service values) of permissible parameter values for each service. For example, permissible parameter ranges are 28.46 for carbon storage (minimum = 0 C kg m^2, maximum = 28.46 C kg m^2) and 73 for stormwater absorption (minimum CN = 98, maximum CN = 25). Dividing PDF ranges by the permissible range for the appropriate service, provides the ratio, or magnitude of uncertain parameter value range ({B} = 0.88, {A} = 0.18, {D} = 0.13 (average for soil types), {C} = 0.09 (average for soil types)) which concurs with the relative order of individual parameter influence. Variation in uncertainty between parameter combinations is relatively consistent between demand measures, as median combined ranges exhibit minor differences, whilst increased variation in maximum combined UES indicator ranges has minimal impact upon the order of uncertainty between parameter combinations.

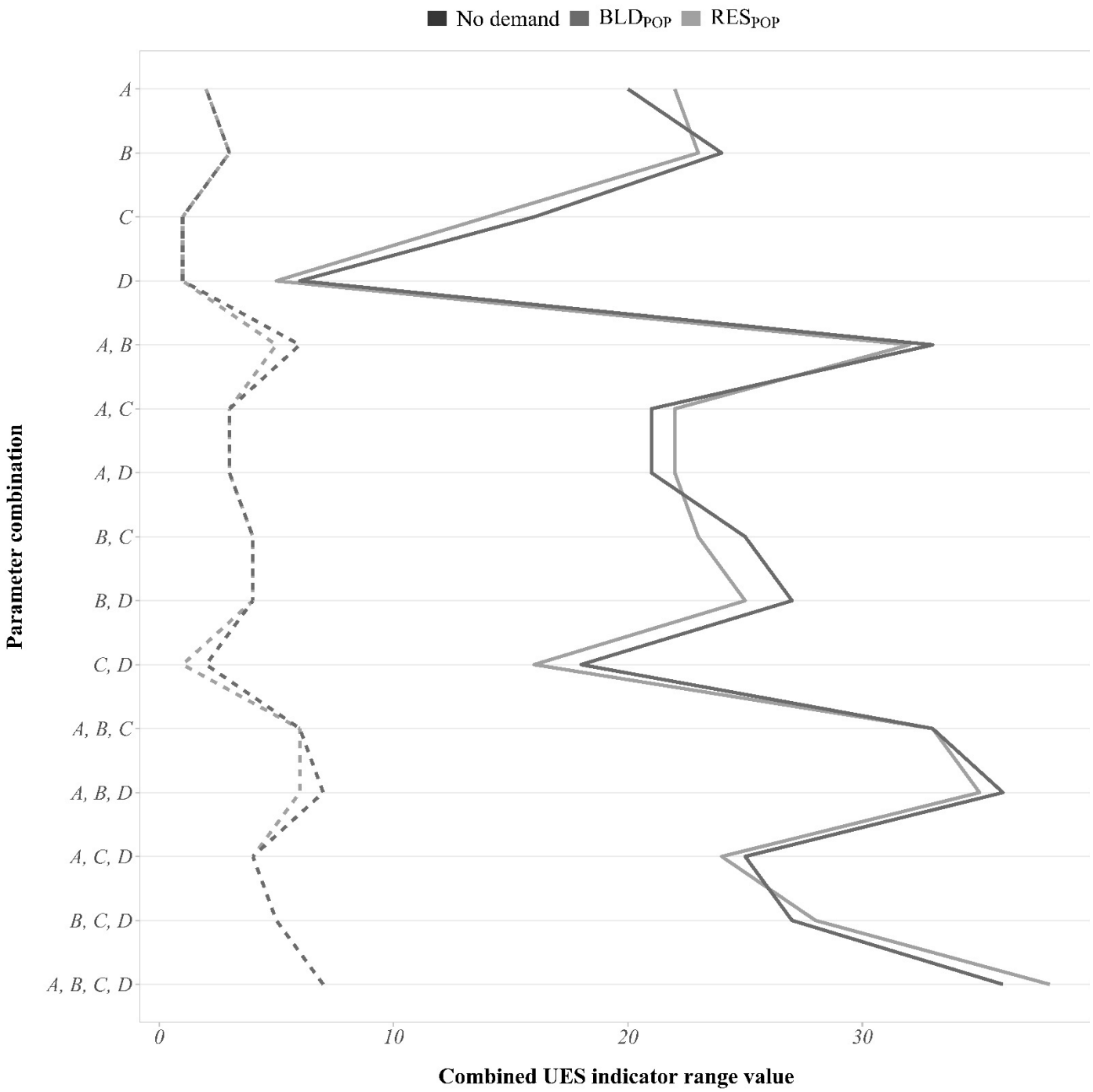

Figure 6 – Median (dashed) and Maximum (solid) range in combined UES indicators for all parameter combinations for all demand weightings

Variation in parameter driven uncertainty between individual cells (**Figure 6**) is thus influenced by variation in cell landcover proportions. **Figure 7** displays landcover proportions, averaged for all cells by unique combined UES indicator range values for each parameter combination (ordered by least [1] to most [15] uncertainty in combined UES values) for No demand cells. A general pattern emerges across all parameter combinations, whereby a single landcover proportion becomes increasingly dominant for cells with relatively higher levels of uncertainty. Tree canopy dominates parameter combination {D}, non-vegetation dominates parameter cobmination {C} and {C,D}, whilst for all subsequent combinations non-tree vegetation increasingly dominates. Interestingly, the patterns for single parameter combinations {D} and {B} are not associated directly to the respective non-tree vegetation and tree canopy uncertain parameters. This may be explained by the dependency of combined UES indicators between cells, as variation in UES parameter values produce a dependency upon the relative ranking index of other cells. Whilst individual cell landcover proportions vary for unique combined UES values, overall patterns indicate that this is not a random spatial process. The figure therefore evidences where high levels of uncertainty in combined UES indicators may occur within the study area.

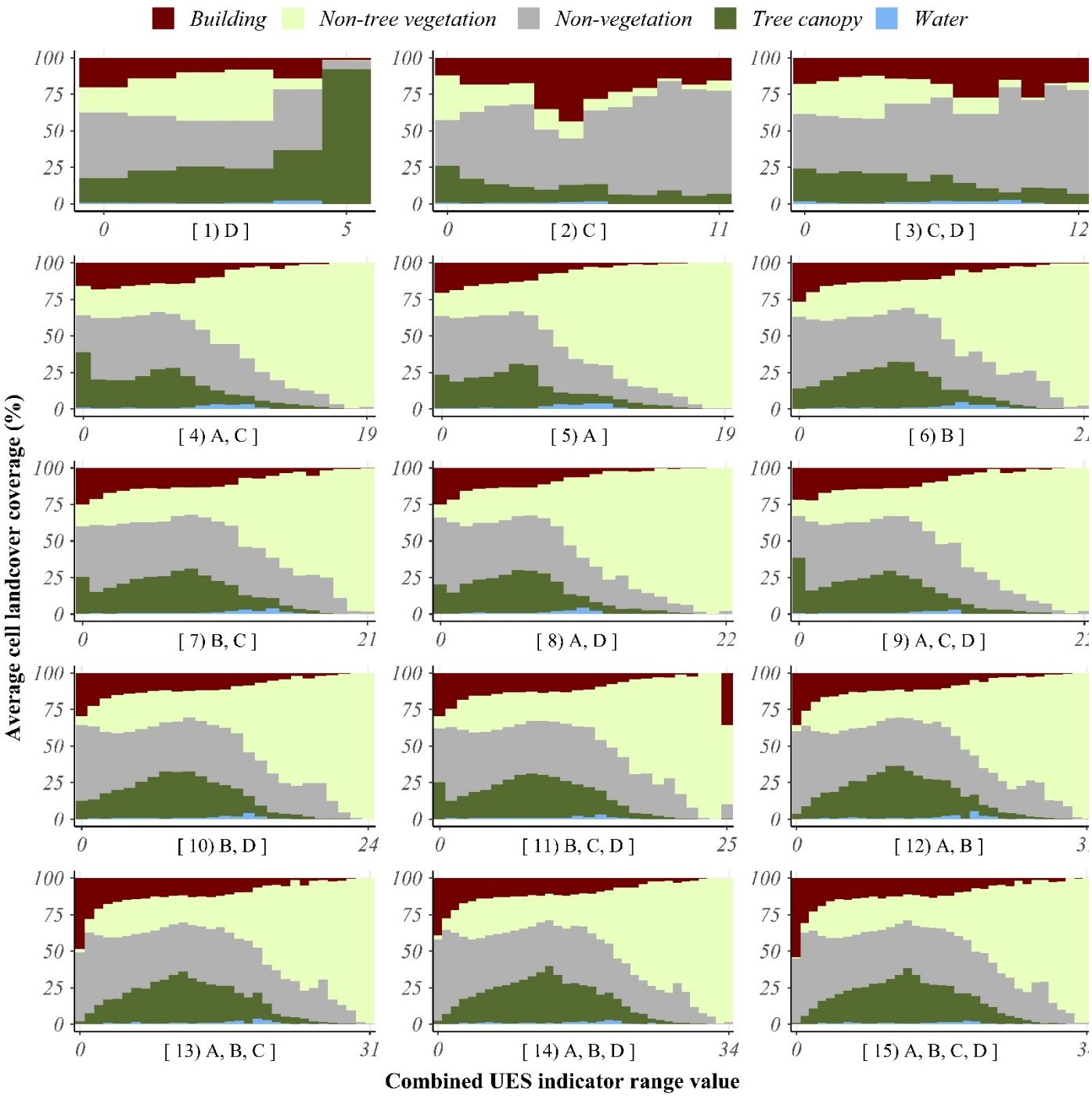

Figure 7 – Average landcover proportions (%) for combined UES indicator range values per parameter combination; designated in order of importance (1 = least importance) within '[ ]' brackets

Parameter uncertainty therefore has some impact upon the identification of coldspots (**Figure 8**). For all cells identified as a coldspot in any parameter setting, over 78% were consistently identified as a final coldspot through overlaying outputs across parameter settings. This percentage differs by 0.8% across all demand weighting methods, indicating relative congruence between UES parameter settings irrespective of varying analysis cell area. Maximum difference in coldspot identification between parameter settings, as a percentage of total coldspot area, is 8.3%, 9.3% and 9.5% for No demand, BLD_{POP} and RES_{POP} cells respectively. Based upon the proxy values used in this study, choice of a particular parameter setting results in a near 10% discrepancy in available coldspot area when compared to maps generated using alternative parameters.

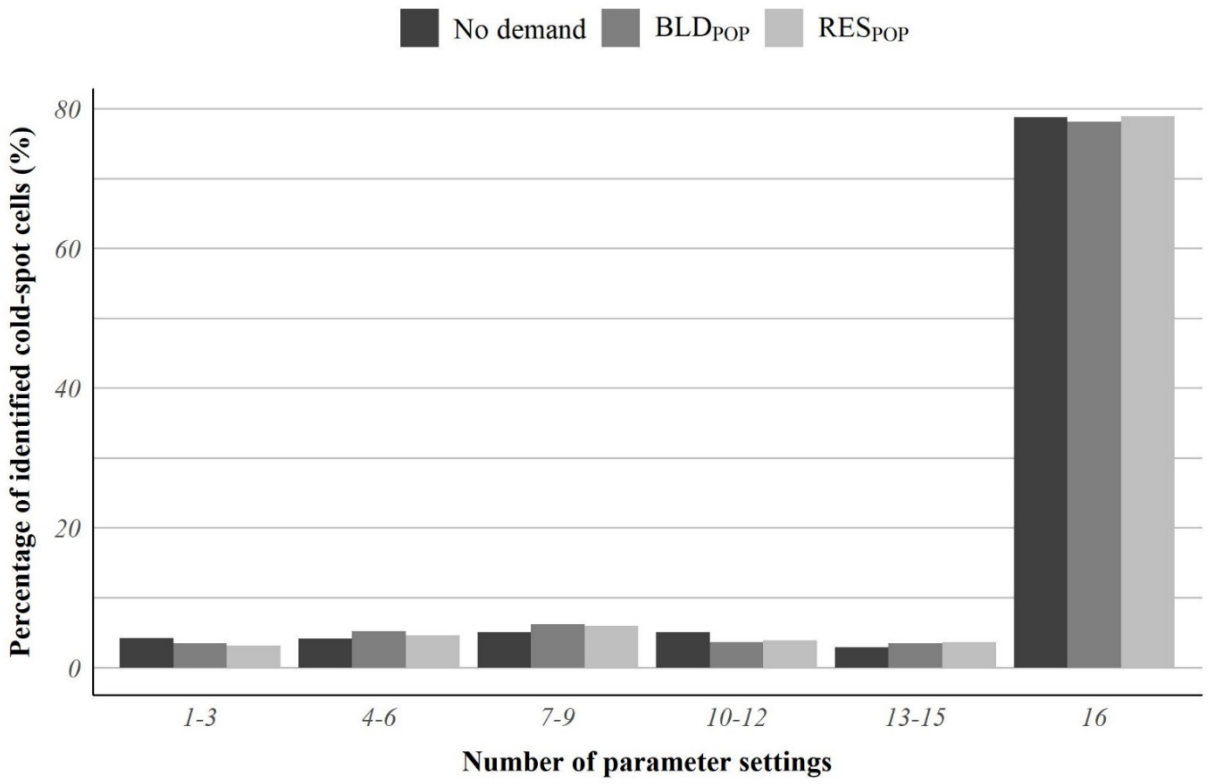

Figure 8 – Number of parameter settings that coldspot cells are identified by demand method

As demonstrated in **Figure 9**, the reduction in the number of demand cells necessarily reduces the total study area percentage identified as a final coldspot from 8.9%, 7% and 5.6% for No demand, BLD_{POP} and RES_{POP} cells respectively. Coldspot clusters are iteratively removed due to this process, which in turn alters the prevalence of deprivation across the study area. The impact of this process is also evident at coarser spatial scales, as altering demand method also results in subtle changes in the identification of deprived ward areas (**Figure 10**). Whilst five out of seven wards are consistently identified as the 20% most UES deprived areas, altering demand measure causes some variation in final map outputs at this spatial scale.

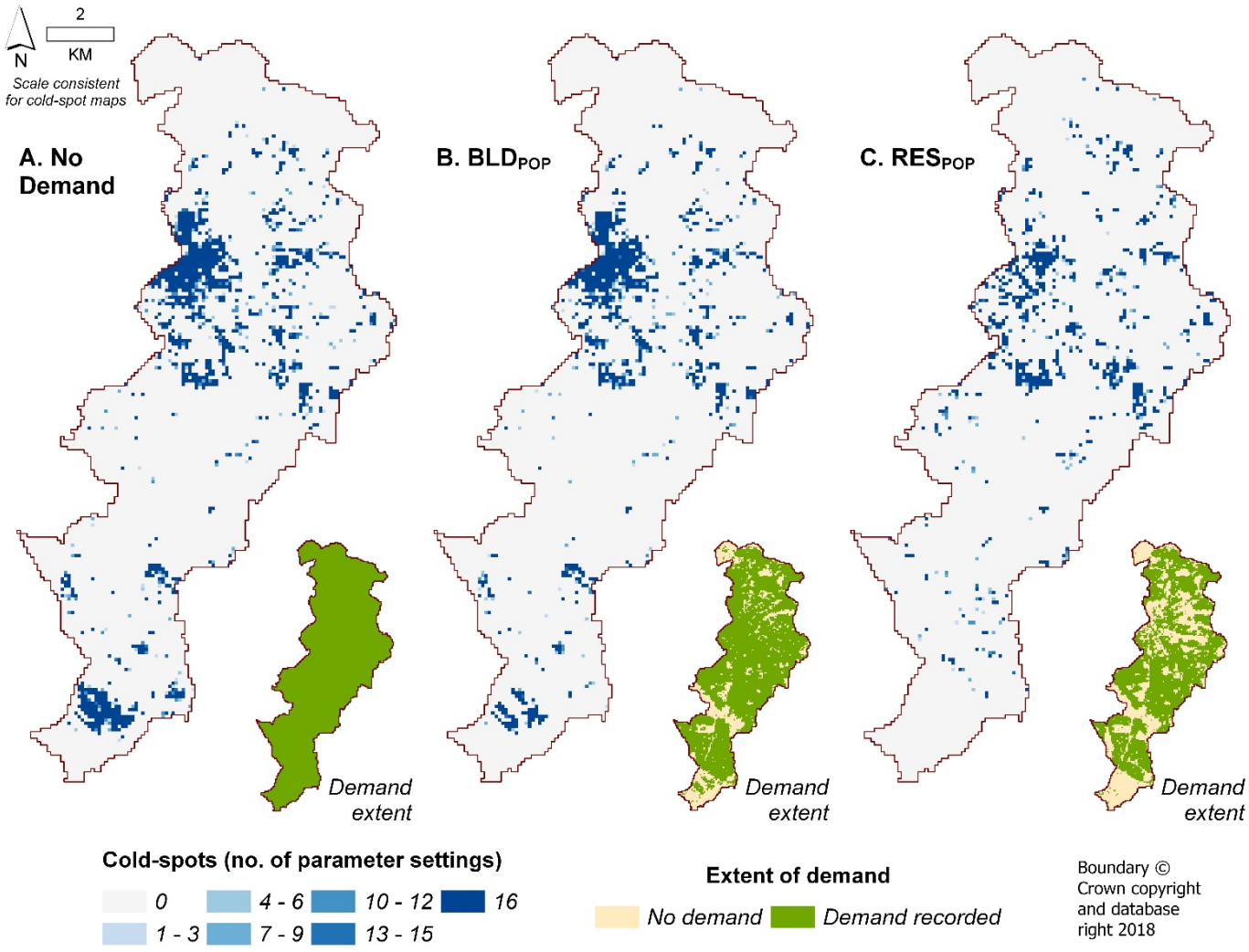

Figure 9 – Overlap of parameter setting coldspots per demand method

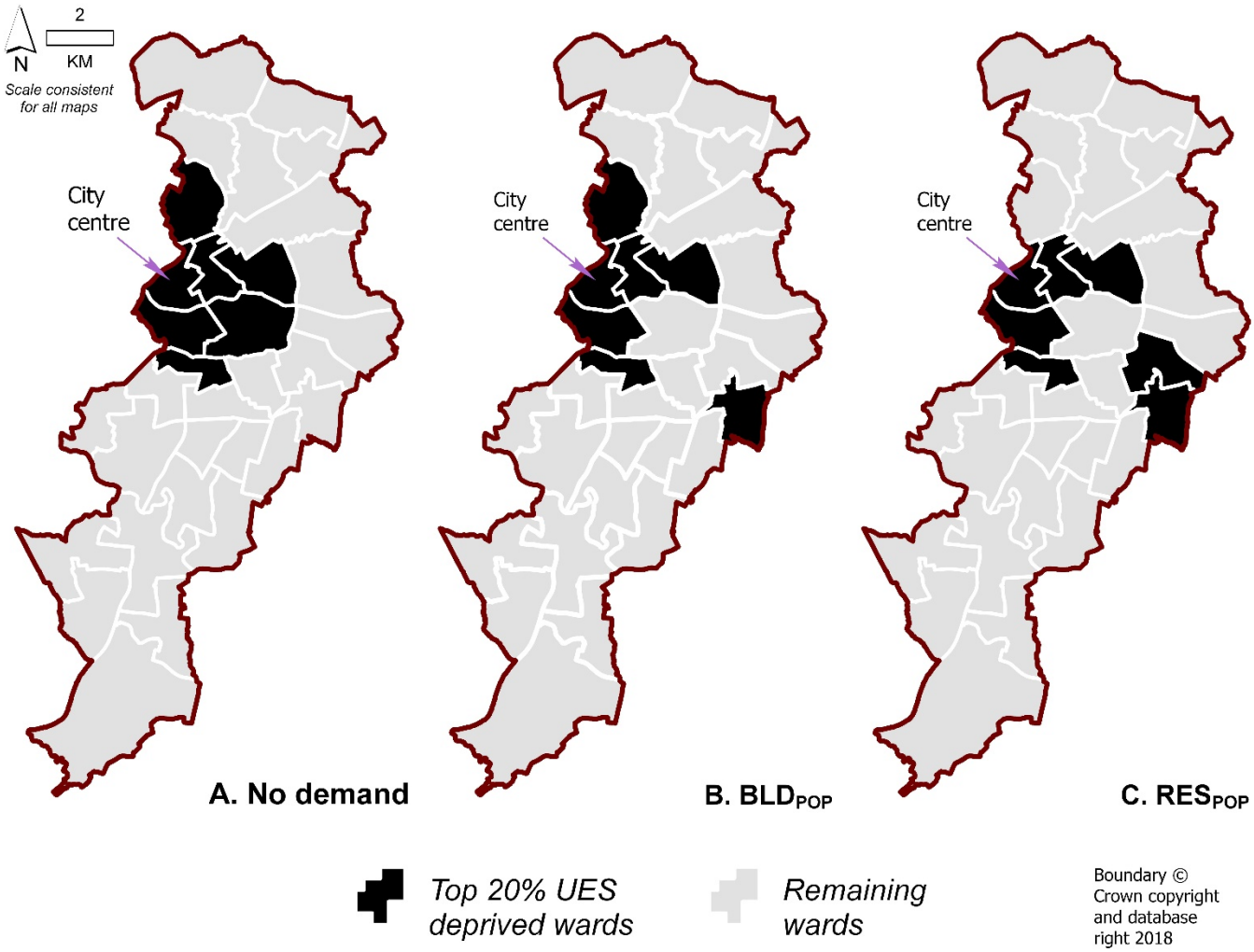

Figure 10 - Top 20% UES deprived wards per demand method

Overall, **Figure 11** demonstrates the resolution of final map products of UES deprivation within the context of both the built environment and administrative ward landscape. It is therefore possible to envisage the type and scale of UGBI investments pragmatically implementable within local neighbourhoods. For example, coldspot areas mainly fall within residential terraced housing areas that overlap administrative ward districts in some areas, in turn providing visual evidence of where ward councils could act collectively to direct local garden greening strategies (Baker et al. 2018).

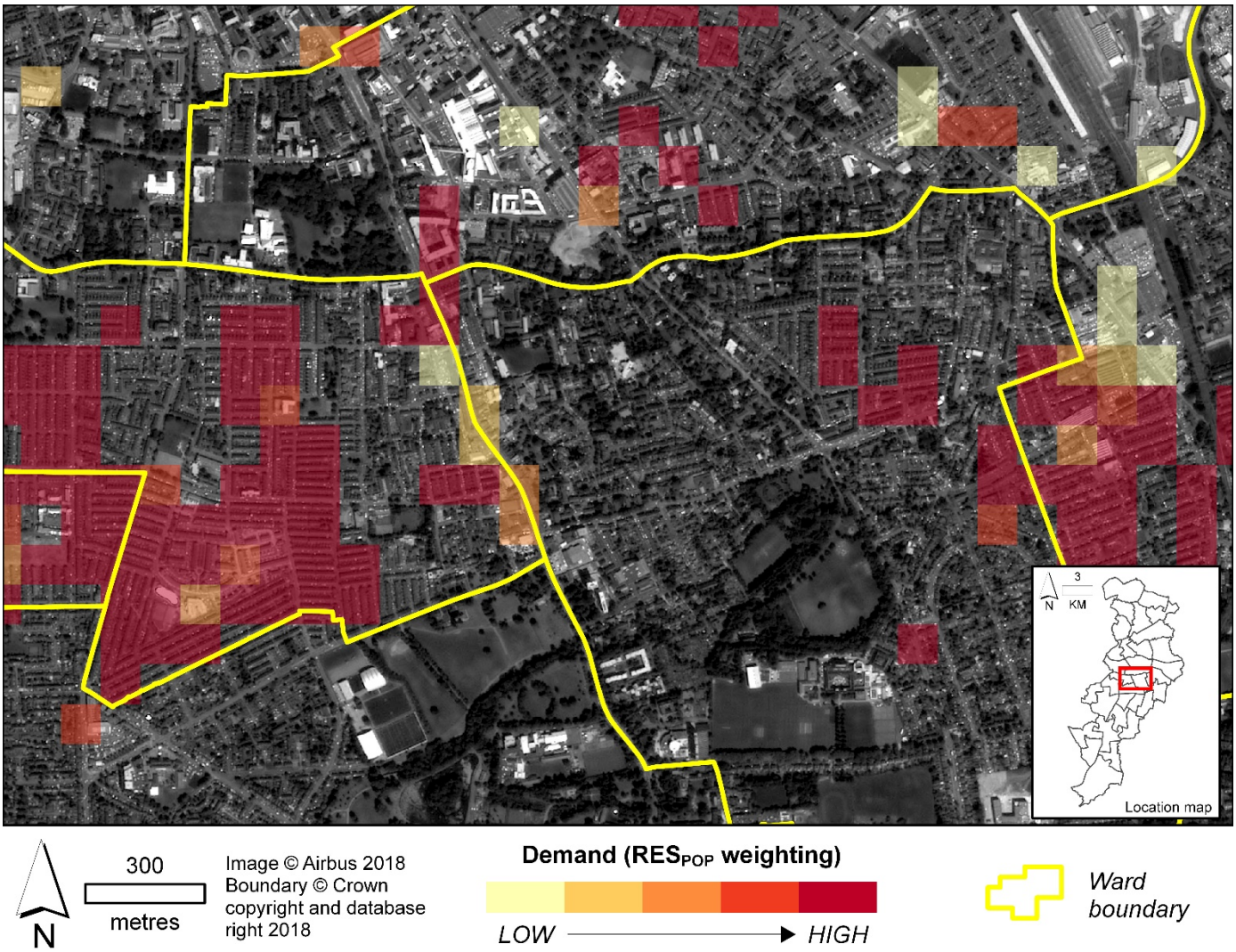

Figure 11 - Visualization of UES coldspots (RES_{POP} demand cells) in relation to urban morphology

4. Discussion

This study presents a novel mapping approach to indicate priority locations to reduce resident exposure to climate related hazards. The approach is therefore transferable to other urban areas using accessible geospatial data and methods, with accompanying sensitivity analysis to indicate the impact upon mapping outputs due to pragmatic considerations required of investigators in different urban areas. Given that UES analysis methods are often opaque (e.g. expert based, black box software) or rely on data specific for an urban area (Haas & Ban 2017, Langemeyer et al. 2020) efforts to improve provide basic and adaptable framework to consider UES knowledge transfer between urban areas (Haase et al. 2014, Luederitz et al. 2015). In particular this approach provides additional support to an environmental/ecological scale representation of UES indicators, especially service benefits under consideration flow continuously across heterogeneous urban landscapes (Baró et al. 2016, Langemeyer et al. 2020).

Spatial resolution in regulating UES in this study are thus important to represent UES benefits within the spatial extent of small-scale urban greening solutions (e.g. street tree planting, sustainable urban drainage systems, green walls and roofs) required to effectively retrofit existing urban infrastructure (Carter et al. 2015, Voskamp et al. 2015). Whilst the approach provides limited information on the type of beneficial UGBI resources for each location, it currently indicates UES deprivation at scales where improved in-situ monitoring exercises may be feasibly implemented to investigate appropriate local UGBI investment strategies (e.g. Massoudieh et al. 2017, Skelhorn. et al. 2014). For both demand (e.g. mid-year population estimates) and service estimation (e.g. aerial imagery, national mapping products) the relevant geospatial data is typically updated at frequent intervals, as such there is potential to adapt the mapping approach to monitor UES change (Haas & Ban 2017, Cabral et al. 2016). Service and demand values updated within the fixed analysis grid structure may therefore enable consistent re-examination of UES dynamics according to continual

change in the urban biophysical, socio-economic, and administrative landscape (Dobbs et al. 2018, Schwarz et al. 2011).

In addition to aiding transferability of this approach, novel incorporation of sensitivity analysis provides beneficial insights for further UES research. For example, UES deprivation maps in this approach are highly sensitive to associated demand weightings, that may result in skewed views of UES service/demand dynamics if not considered, such as UES deprivation mapped to no population areas such as airport runways, large car parks etc. The findings thus serve to raise further awareness as to the benefits of including demand measures in wider UES research, particularly where UES flows exhibit high levels of spatial dependency at the micro-scale (Baró et al. 2016, Larondelle & Lauf 2016). The various quality of UES deprivation maps in turn provide a general indication as to whether data for a particular demand method, using this or a similar approach, is worth the investment in resources to meet a desired level of analysis in further case studies.

In addition, as proxy models remain a popular choice in UES mapping approaches, sensitivity analysis indicates that increasing relative magnitudes in proxy parameter uncertainty may reflect uncertainty in mapping outputs when applied linearly to landcover area estimates. This is evidently a spatially dependent process that becomes increasingly complex as additional sources of landcover associated uncertainty are compounded within aggregated UES indicators. Variation in map uncertainty across the study area therefore varies widely and may apply to other approaches that use similar methods in proxy to landcover extrapolation (Zhao & Sander 2018). Due to interdependencies in landcover proportions per cell, associated uncertainty is difficult to model using standard statistical techniques. Therefore, overlapping findings, obtained from different interactions in uncertain inputs, can provide an easy to implement consensus view of combined UES indicators (Eigenbrod et al. 2010, Schröter & Remme 2016), and should be implemented to examine parameter uncertainty due to aforementioned complexities in spatial uncertainty estimation.

Despite benefits to sensitivity analysis, some limitations in proxy based UES methods remain, as the lack of independent validation to primary data results limits understanding of remaining uncertainty within current mapping outputs (Eigenbrod et al. 2010, Zhao & Sander 2018). Efforts to address this issue may therefore begin with improvements in the thematic resolution of landcover data from use of ancillary information in the classification process (e.g. multi-spectral imagery, LiDAR; Baker et al. 2018, Dennis et al. 2018). For example, stratification of non-tree vegetation into grass and bush categories, and tree canopies according to canopy height, can support extrapolation of independent field sample carbon storage estimates of local vegetation types for these categories (Davies et al. 2011, Raciti et al. 2014). Improved landcover data could also be incorporated with topographical elevation and underground drainage data to support both advanced hydraulic modelling of UGBI flooding reduction within urbanised catchments (Sjöman et al. 2013), in addition to high resolution climate models to assess UGBI impacts upon localised temperatures under various heatwave scenarios (Skelhorn et al. 2014).

Models validated to local environmental conditions have been employed successfully to examine UGBI benefits at various scales of analysis. However, the associated resource investments (e.g. software, primary data) required are typically prohibitive for entire urban areas when multiple UES are concerned (Kremer et al. 2016b). Where use of proxy methods is unavoidable, uncertainty may be further addressed through UGBI and landcover categorisations designed for appropriate UES indicator transfer from suitably chosen proxies (Andrew et al. 2015, Derkzen et al. 2015). In relation to regression techniques for temperature regulation, improved landcover categorisation and use of additional variables such as landscape metrics, tree/building shading, and elevation for example, may also improve the accuracy of validated temperature regulation UES estimates (Chen et al. 2014, Kong et al. 2014). Demand indicators may be further updated to accommodate localised exposure to environmental hazards (i.e. exposure to extreme temperatures, pluvial/fluvial flooding

risks) in addition to vulnerability factors within the local population (i.e. age, mobility, economic situation) (Jenerette et al. 2016, Kaźmierczak & Cavan 2011). In addition, as service benefits may flow outside single cell areas (i.e. runoff from neighbouring areas could flow into, and thus increase flooding risks for cell residents) the regular analysis grid structure should prove useful to investigate service to demand dynamics at various spatial scales of benefit transfer (Baró et al. 2016).

Future research may therefore consider validation of uncertainty in popular UES proxy methods using samples of primary data, and/or models validated by primary data at sample locations (Eigenbrod et al. 2010). In addition, extensions to sensitivity should be considered in future studies for other sources of uncertainty such as landcover misclassification errors (Convertino et al. 2013), importance weighting of individual UES according to stakeholder needs (Kremer et al. 2016a), in addition to parameterisation uncertainties for additional UES models within the mapping approach. Whilst parameter comparison enabled consideration of spatially dependent interactions between all uncertain parameter combinations, this method will become less computationally feasible when considering additional sources of uncertainty. Variance based global sensitivity analysis have been successfully applied to examine complex interactions between multiple sources of uncertainty in spatial models (Convertino et al. 2013, Lilburne & Tarantola 2009) and may therefore provide a pragmatic solution in this respect. Further examination of this, and other sensitivity/uncertainty analyses is therefore required to improve standardisation of uncertainty estimation for various UES indicator metrics/prioritisation measures (Hou et al. 2013, Schröter & Remme 2016), and is ultimately required to improve communication of the overall usability of UES maps to end users. The case study here therefore explicitly considered realistic pragmatic difficulties in current citywide UES mapping exercises with the intention to guide further research efforts towards this goal.

5. Conclusion

The mapping approach presented in this study, presents a transferable methodology to investigate how current regulating UES fulfils service demand amongst the local urban population. This approach ultimately provides a trade-off between coarse-scale UES mapping studies where demand from Landuse/Landcover categorisations, or within municipal districts are explicitly considered (Baró et al. 2017, Haas & Ban 2017) to gridded approaches employed at the ecological/environmental scale (Dobbs et al. 2018, Kremer et al. 2016a). As financial resources for UGBI improvement may be constrained, UES deprivation analysis in the mapping approach usefully indicates areas of greatest concern for potential UGBI investment.

Sensitivity analysis in this study proved vital to demonstrate the wide-ranging issues in proxy model implementation for UES mapping studies in general. Explicit examination of uncertainty in proxy methods is useful not only to guide application of the mapping approach for different urban areas, but usefully conveys the overall usability of the mapping outputs for further planning purposes (Haase et al. 2014, Luederitz et al. 2015). Such efforts are thus beneficial to assess and re-appraise issues in current UES mapping methods, to aid the development of consistent and standardised approaches for mapping UES (Seppelt et al. 2011).

In the wider context, the development of UES mapping approaches is useful for highlighting the applicability of urban UES mapping data for urban planning purposes. It is hoped that this raises awareness and encourages investment in improved environmental modelling software, smart-city monitoring networks (e.g. local temperatures, pollution levels) and mapping data (e.g. high spatial-resolution imagery, three-dimensional data) to better facilitate validated UES analysis, and thus improve provision of regulating UES in urban areas (Schröter et al. 2014, Zhao & Sander 2018). This

improvement will greatly assist efforts to improve our towns and cities resilience to environmental hazards now and in uncertain future climate conditions.

Acknowledgements

This research was funded by Manchester Metropolitan University and UNIGIS UK. We kindly thank the Ordnance Survey for licensing the AddressBase product for our research. We also kindly thank the independents reviewers for the time and effort for the invaluable comments regarding the manuscript.

6. References

Anderson, B.J., Armsworth, P.R., Eigenbrod, F., Thomas, C.D., Gillings, S., Heinemeyer, A., Roy, D.B. and Gaston, K.J. (2009). Spatial covariance between biodiversity and other ecosystem service priorities. *Journal of Applied Ecology*, *46* (4), 888-896.

Andrew, M. E., Wulder, M. A., Nelson, T. A., & Coops, N. C. (2015). Spatial data, analysis approaches, and information needs for spatial ecosystem service assessments: a review. *GIScience & Remote Sensing*, *52* (3), 344-373.

Baker, F., Smith, C., & Cavan, G. (2018). A combined approach to classifying land surface cover of urban domestic gardens using citizen science data and high resolution image analysis. *Remote Sensing*, *10* (4), 537.

Baró, F., Palomo, I., Zulian, G., Vizcaino, P., Haase, D., & Gómez-Baggethun, E. (2016). Mapping ecosystem service capacity, flow and demand for landscape and urban planning: A case study in the Barcelona metropolitan region. *Land use policy*, *57*, 405-417.

Baró, F., Gómez-Baggethun, E., & Haase, D. (2017). Ecosystem service bundles along the urban-rural gradient: Insights for landscape planning and management. *Ecosystem services*, *24*, 147-159.

Bhaduri, B., Bright, E., Coleman, P., & Urban, M. L. (2007). LandScan USA: a high-resolution geospatial and temporal modeling approach for population distribution and dynamics. *GeoJournal*, *69* (1-2), 103-117.

Cabral, P., Feger, C., Levrel, H., Chambolle, M., & Basque, D. (2016). Assessing the impact of land-cover changes on ecosystem services: A first step toward integrative planning in Bordeaux, France. *Ecosystem Services*, *22*, 318-327.

Carter, J. G., Cavan, G., Connelly, A., Guy, S., Handley, J., & Kazmierczak, A. (2015). Climate change and the city: Building capacity for urban adaptation. *Progress in planning*, *95*, 1-66.

Chen, A., Yao, X. A., Sun, R., & Chen, L. (2014). Effect of urban green patterns on surface urban cool islands and its seasonal variations. *Urban forestry & urban greening*, *13*(4), 646-654.

CityOfTrees (2011); Greater Manchester Tree Audit, Manchester, UK. Personal communication.

Convertino, M., Muñoz-Carpena, R., Chu-Agor, M. L., Kiker, G. A., & Linkov, I. (2014). Untangling drivers of species distributions: Global sensitivity and uncertainty analyses of MaxEnt. *Environmental Modelling & Software*, *51*, 296-309.

Coseo, P., & Larsen, L. (2014). How factors of land use/land cover, building configuration, and adjacent heat sources and sinks explain Urban Heat Islands in Chicago. *Landscape and Urban Planning*, *125*, 117-129.

Cranfield University (2018). LandIS: Land Information System. Available online: http://www.landis.org.uk/, September, 2018.

Cruickshank, M. M., Tomlinson, R. W., Devine, P. M., & Milne, R. (1998, August). Carbon in the vegetation and soils of Northern Ireland. In *Biology and Environment: Proceedings of the Royal Irish Academy* (pp. 9-21). Royal Irish Academy.

Davies, Z. G., Edmondson, J. L., Heinemeyer, A., Leake, J. R., & Gaston, K. J. (2011). Mapping an urban ecosystem service: quantifying above-ground carbon storage at a city-wide scale. *Journal of applied ecology*, *48*(5), 1125-1134.

Dennis, M., Barlow, D., Cavan, G., Cook, P., Gilchrist, A., Handley, J., James, P., Thompson, J., Tzoulas, K., Wheater, C.P. and Lindley, S. (2018). Mapping urban green infrastructure: A novel

landscape-based approach to incorporating land use and land cover in the mapping of human-dominated systems. *Land*, *7*(1), 17.

Derkzen, M. L., van Teeffelen, A. J., & Verburg, P. H. (2015). Quantifying urban ecosystem services based on high-resolution data of urban green space: an assessment for Rotterdam, the Netherlands. *Journal of Applied Ecology*, *52*(4), 1020-1032.

Dobbs, C., Hernández-Moreno, Á., Reyes-Paecke, S., & Miranda, M. D. (2018). Exploring temporal dynamics of urban ecosystem services in Latin America: The case of Bogota (Colombia) and Santiago (Chile). *Ecological Indicators*, *85*, 1068-1080.

Edina Digimap (2017). Ordnance Survey. Available online: https://digimap.edina.ac.uk/os, (accessed May, 2017)

Eigenbrod, F., Armsworth, P.R., Anderson, B.J., Heinemeyer, A., Gillings, S., Roy, D.B., Thomas, C.D. and Gaston, K.J (2010). The impact of proxy-based methods on mapping the distribution of ecosystem services. *Journal of Applied Ecology*, *47*(2), 377-385.

Getmapping, Aerial Data (2017) High Resolution Imagery. Available online: http://www.getmapping.com/products-and-services/aerial-imagery-data/aerial-data-high-resolution-imagery (accessed on 29 March 2018)

Gill, S. E., Handley, J. F., Ennos, A. R., & Pauleit, S. (2007). Adapting cities for climate change: the role of the green infrastructure. *Built environment*, *33*(1), 115-133.

Gómez-Baggethun, E., & Barton, D. N. (2013). Classifying and valuing ecosystem services for urban planning. *Ecological economics*, *86*, 235-245.

Haas, J., & Ban, Y. (2017). Mapping and monitoring urban ecosystem services using multitemporal high-resolution satellite data. *IEEE Journal of Selected Topics in Applied Earth Observations and Remote Sensing*, *10*(2), 669-680.

Haase, D., Larondelle, N., Andersson, E., Artmann, M., Borgström, S., Breuste, J., Gomez-Baggethun, E., Gren, Å., Hamstead, Z., Hansen, R. and Kabisch, N. (2014). A quantitative review of urban ecosystem service assessments: concepts, models, and implementation. *Ambio*, *43*(4), 413-433.

Hall, J. M., Handley, J. F., & Ennos, A. R. (2012). The potential of tree planting to climate-proof high density residential areas in Manchester, UK. *Landscape and Urban Planning*, *104*(3-4), 410-417.

Harlan, S., Chowell, G., Yang, S., Petitti, D., Morales Butler, E., Ruddell, B., & Ruddell, D. (2014). Heat-related deaths in hot cities: estimates of human tolerance to high temperature thresholds. *International journal of environmental research and public health*, *11*(3), 3304-3326.

Holt, A. R., Mears, M., Maltby, L., & Warren, P. (2015). Understanding spatial patterns in the production of multiple urban ecosystem services. *Ecosystem services*, *16*, 33-46.

Hou, Y., Burkhard, B., & Müller, F. (2013). Uncertainties in landscape analysis and ecosystem service assessment. *Journal of environmental management*, *127*, S117-S131.

Jenerette, G.D., Harlan, S.L., Buyantuev, A., Stefanov, W.L., Declet-Barreto, J., Ruddell, B.L., Myint, S.W., Kaplan, S. and Li, X. (2016). Micro-scale urban surface temperatures are related to land-cover features and residential heat related health impacts in Phoenix, AZ USA. *Landscape Ecology*, *31*(4), 745-760.

Jia, P., Qiu, Y., & Gaughan, A. E. (2014). A fine-scale spatial population distribution on the high-resolution gridded population surface and application in Alachua County, Florida. *Applied Geography*, *50*, 99-107.

Kabisch, N., Frantzeskaki, N., Pauleit, S., Naumann, S., Davis, M., Artmann, M., Haase, D., Knapp, S., Korn, H., Stadler, J. and Zaunberger, K. (2016). Nature-based solutions to climate change mitigation and adaptation in urban areas: perspectives on indicators, knowledge gaps, barriers, and opportunities for action. *Ecology and Society*, *21*(2).

Kaźmierczak, A., & Cavan, G. (2011). Surface water flooding risk to urban communities: Analysis of vulnerability, hazard and exposure. *Landscape and Urban Planning*, *103*(2), 185-197.

Kong, F., Yin, H., James, P., Hutyra, L. R., & He, H. S. (2014). Effects of spatial pattern of greenspace on urban cooling in a large metropolitan area of eastern China. *Landscape and Urban Planning*, *128*, 35-47.

Kremer, P., Hamstead, Z. A., & McPhearson, T. (2016a). The value of urban ecosystem services in New York City: A spatially explicit multicriteria analysis of landscape scale valuation scenarios. *Environmental Science & Policy*, *62*, 57-68.

Kremer, P., Hamstead, Z., Haase, D., McPhearson, T., Frantzeskaki, N., Andersson, E., Kabisch, N., Larondelle, N., Rall, E.L., Voigt, A. and Baró, F. (2016b). Key insights for the future of urban ecosystem services research. *Ecology and Society* 21 (2), 29.

Kroll, F., Müller, F., Haase, D., & Fohrer, N. (2012). Rural–urban gradient analysis of ecosystem services supply and demand dynamics. *Land use policy*, *29* (3), 521-535.

Laaidi, K., Zeghnoun, A., Dousset, B., Bretin, P., Vandentorren, S., Giraudet, E., & Beaudeau, P. (2011). The impact of heat islands on mortality in Paris during the August 2003 heat wave. *Environmental health perspectives*, *120* (2), 254-259.

Langemeyer, J., Wedgwood, D., McPhearson, T., Baró, F., Madsen, A. L., & Barton, D. N. (2020). Creating urban green infrastructure where it is needed–A spatial ecosystem service-based decision analysis of green roofs in Barcelona. *Science of the Total Environment*, *707*, 135487.

Larondelle, N., & Lauf, S. (2016). Balancing demand and supply of multiple urban ecosystem services on different spatial scales. *Ecosystem Services*, *22*, 18-31.

Lilburne, L., & Tarantola, S. (2009). Sensitivity analysis of spatial models. *International Journal of Geographical Information Science*, *23*(2), 151-168.

Luederitz, C., Brink, E., Gralla, F., Hermelingmeier, V., Meyer, M., Niven, L., ... & Abson, D. J. (2015). A review of urban ecosystem services: six key challenges for future research. *Ecosystem services*, *14*, 98-112.

Massoudieh, A., Maghrebi, M., Kamrani, B., Nietch, C., Tryby, M., Aflaki, S., & Panguluri, S. (2017). A flexible modeling framework for hydraulic and water quality performance assessment of stormwater green infrastructure. *Environmental modelling & software*, *92*, 57-73.

MCC [Manchester City Council] (2018). Population: Manchester's population, ethnicity and migration. Retrieved from https://secure.manchester.gov.uk/info/200088/statistics_and_intelligence/438/population, July, 2018

Muller, C. L., Chapman, L., Grimmond, C. S. B., Young, D. T., & Cai, X. (2013). Sensors and the city: a review of urban meteorological networks. *International Journal of Climatology*, *33*(7), 1585-1600.

O'Brien, O., & Cheshire, J. (2016). Interactive mapping for large, open demographic data sets using familiar geographical features. *Journal of Maps*, *12*(4), 676-683.

Oke, T. R. (1988). *Boundary layer climates*. Routledge.

OS [Ordnance Survey] (2018). Addressbase Products. Available online: https://www.ordnancesurvey.co.uk/business-and-government/products/addressbase-products.html, May 2018

Plummer, M. L. (2009). Assessing benefit transfer for the valuation of ecosystem services. *Frontiers in Ecology and the Environment*, *7*(1), 38-45.

Pulighe, G., Fava, F., & Lupia, F. (2016). Insights and opportunities from mapping ecosystem services of urban green spaces and potentials in planning. *Ecosystem services*, *22*, 1-10..

Salvadore, E., Bronders, J., & Batelaan, O. (2015). Hydrological modelling of urbanized catchments: A review and future directions. *Journal of hydrology*, *529*, 62-81.

Schröter, M., Remme, R. P., Sumarga, E., Barton, D. N., & Hein, L. (2015). Lessons learned for spatial modelling of ecosystem services in support of ecosystem accounting. *Ecosystem Services*, *13*, 64-69.

Schröter, M., & Remme, R. P. (2016). Spatial prioritisation for conserving ecosystem services: comparing hotspots with heuristic optimisation. *Landscape ecology*, *31*(2), 431-450.

Schulp, C. J., Burkhard, B., Maes, J., Van Vliet, J., & Verburg, P. H. (2014). Uncertainties in ecosystem service maps: a comparison on the European scale. *PloS one*, *9*(10), e109643.

Schwarz, N., Bauer, A., & Haase, D. (2011). Assessing climate impacts of planning policies—an estimation for the urban region of Leipzig (Germany). *Environmental impact assessment review*, *31*(2), 97-111.

Seppelt, R., Dormann, C. F., Eppink, F. V., Lautenbach, S., & Schmidt, S. (2011). A quantitative review of ecosystem service studies: approaches, shortcomings and the road ahead. *Journal of Applied Ecology*, *48*(3), 630-636

Sjöman, J. D., & Gill, S. E. (2014). Residential runoff–The role of spatial density and surface cover, with a case study in the Höjeå river catchment, southern Sweden. *Urban forestry & urban greening*, *13*(2), 304-314.

Skelhorn, C., Lindley, S., & Levermore, G. (2014). The impact of vegetation types on air and surface temperatures in a temperate city: A fine scale assessment in Manchester, UK. *Landscape and Urban Planning*, *121*, 129-140.

Stevens, F. R., Gaughan, A. E., Linard, C., & Tatem, A. J. (2015). Disaggregating census data for population mapping using random forests with remotely-sensed and ancillary data. *PloS one*, *10*(2), e0107042.

UKDS [UK Data Service] (2017). Census Boundary Data. Retrieved from https://www.ukdataservice.ac.uk/, April, 2017.

USDA [United States Department of Agriculture, Soil Conservation Society] (1986). Urban hydrology for small watersheds. *Technical release*, *55*, 2-6.

USGS [United States Geological Survey] (2017). Earth Explorer Service. Available online: https://earthexplorer.usgs.gov/, September 2017

Voskamp, I. M., & Van de Ven, F. H. (2015). Planning support system for climate adaptation: Composing effective sets of blue-green measures to reduce urban vulnerability to extreme weather events. *Building and Environment*, *83*, 159-167.

Wang, F., Qin, Z., Song, C., Tu, L., Karnieli, A., & Zhao, S. (2015). An improved mono-window algorithm for land surface temperature retrieval from Landsat 8 thermal infrared sensor data. *Remote Sensing*, *7*(4), 4268-4289.

Weather Underground (2017). Manchester Airport, GB. Available online: https://www.wunderground.com/weather/EGCC, September 2017

Woodruff, S. C., & BenDor, T. K. (2016). Ecosystem services in urban planning: Comparative paradigms and guidelines for high quality plans. *Landscape and Urban Planning*, *152*, 90-100.

Zandbergen, P. A. (2011). Dasymetric mapping using high resolution address point datasets. *Transactions in GIS*, *15*, 5-27.

Zandbergen, P. A., & Ignizio, D. A. (2010). Comparison of dasymetric mapping techniques for small-area population estimates. *Cartography and Geographic Information Science*, *37*(3), 199-214.

Zhao, C., & Sander, H. A. (2018). Assessing the sensitivity of urban ecosystem service maps to input spatial data resolution and method choice. *Landscape and urban planning*, *175*, 11-22.

Appendix 1: Population disaggregation workflows

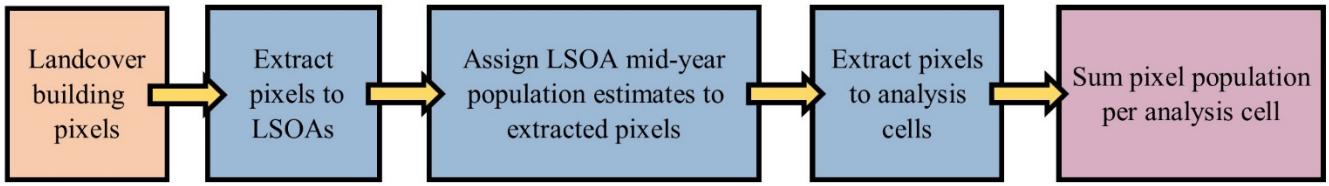

BLD$_{POP}$ weighting workflow

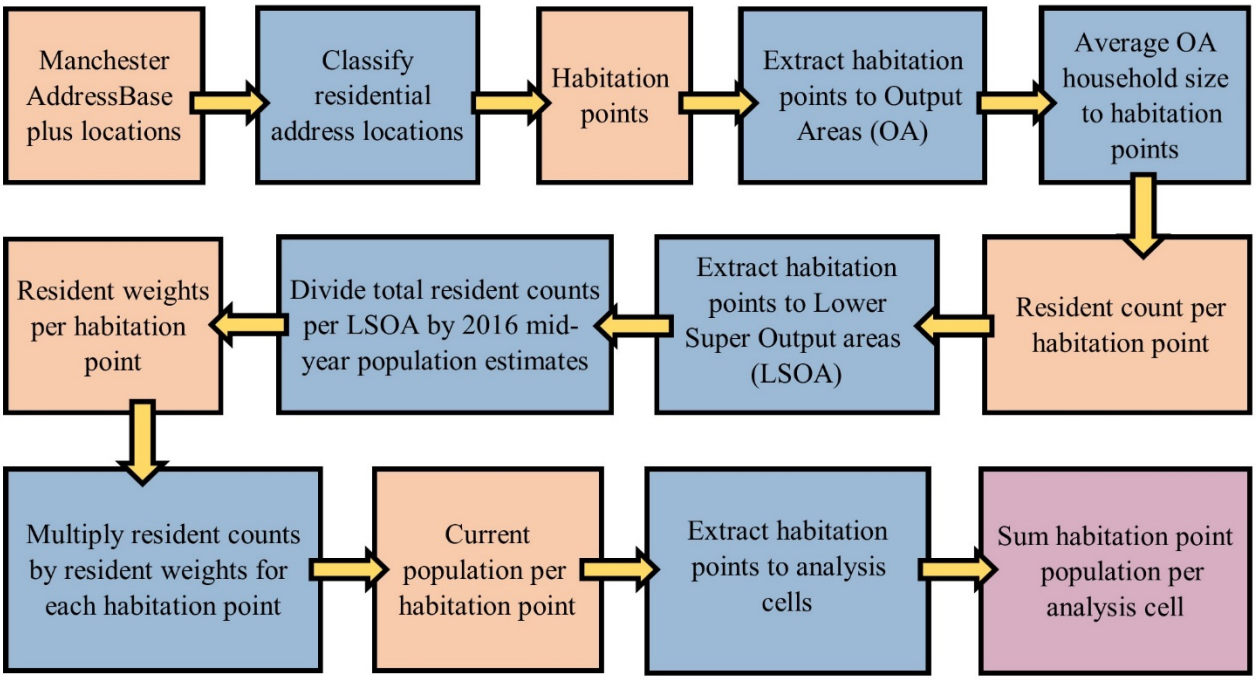

RES$_{POP}$ weighting workflow

Notes:

Output areas and Lower Super Output areas represent statistical spatial measurement areas in the 2011 UK census (Retrieved from UK Data Service, https://www.ukdataservice.ac.uk/, accessed 2017). Output areas represent resident population groupings averaging 309 people. Lower Super Output areas contain multiple Output areas with average of 1500 people. 2016 LSOA mid-year population estimates from the UK Office of National Statistics (ONS) are for Lower super output areas (Retrieved from ONS,

https://www.ons.gov.uk/peoplepopulationandcommunity/populationandmigration/populationestimates/bulletins/annualmidyearpopulationestimates/latest , Accessed 2018). Household size estimates at Output Area level are drawn from the UK 2011 census (Retrieved from ONS: Nomisweb, https://www.nomisweb.co.uk/, accessed 2017).

Appendix 2: Temperature regulation & Demand indicators

NOTE:

The following figures show the distribution of indicator values for all UES parameter settings and demand methods.

Indicator values are thus classified into equal number indicator deciles.

No demand cells are where demand weighted population < 1.

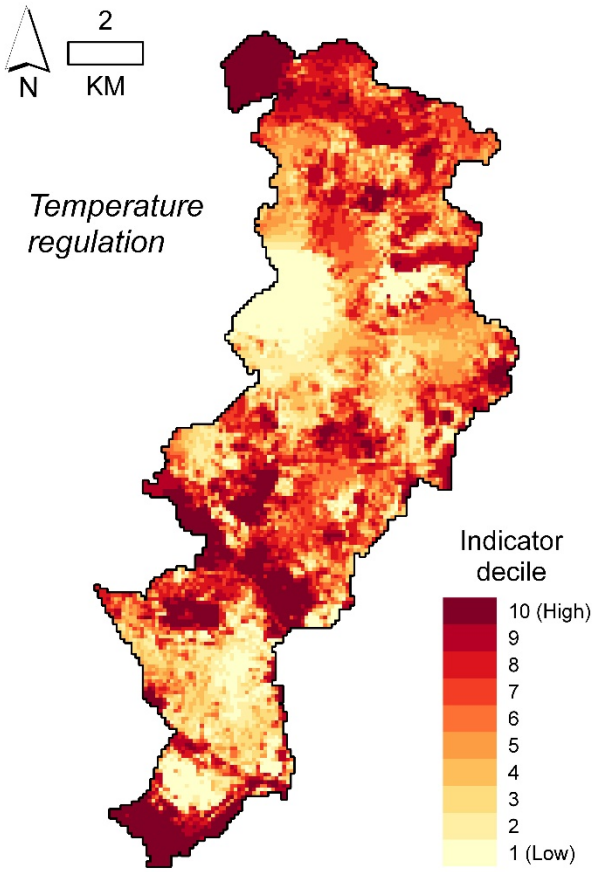

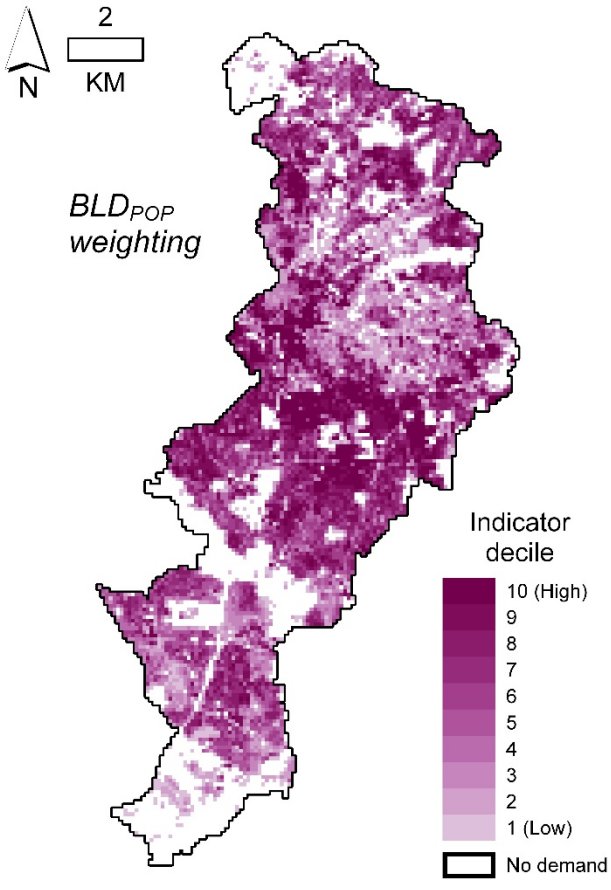

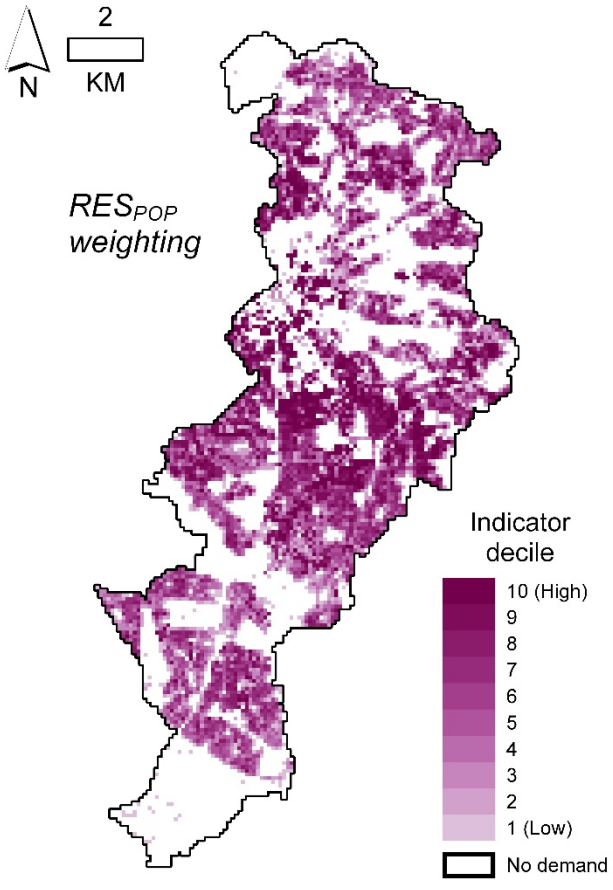

Appendix 2: Carbon Storage indicators

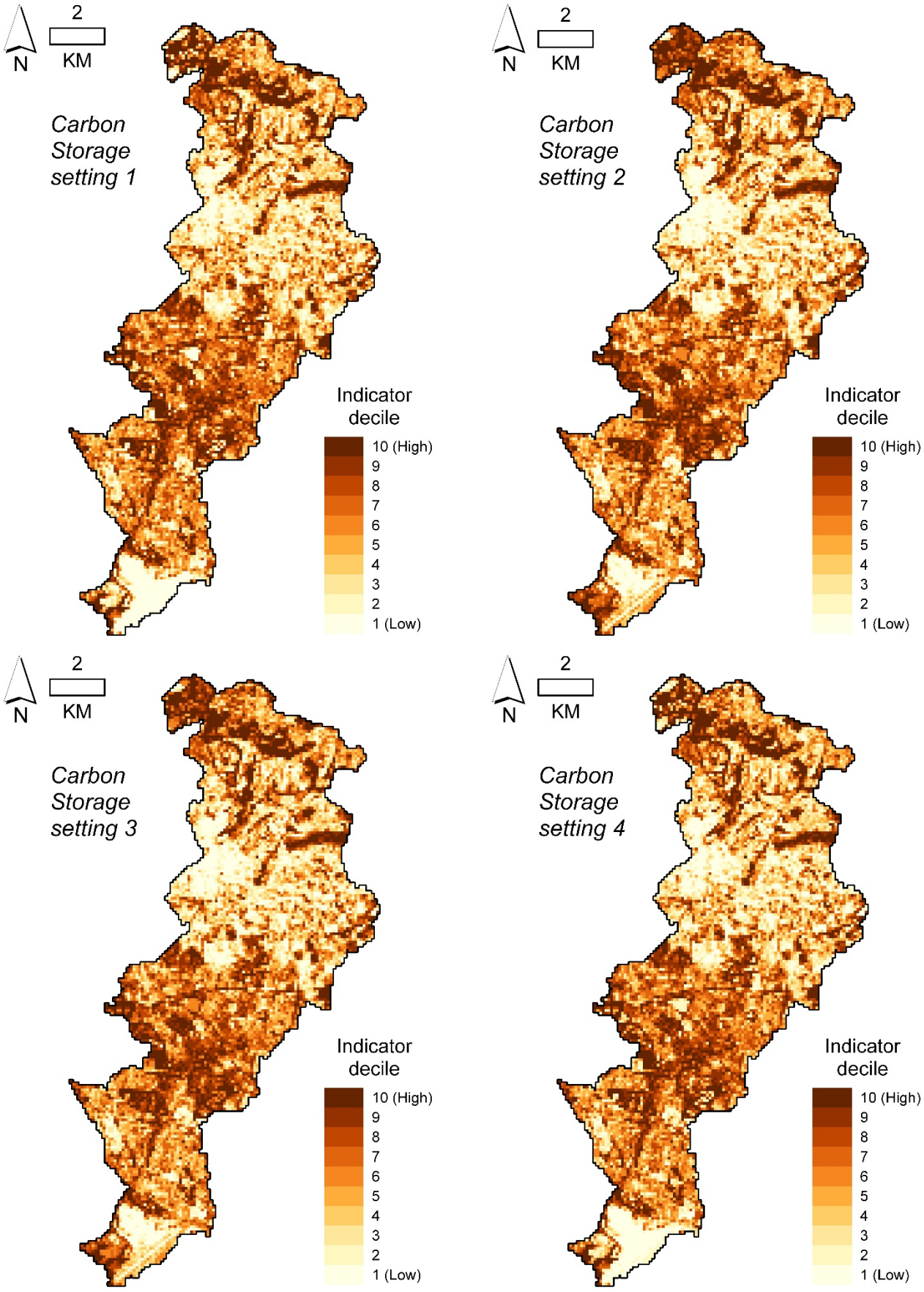

Appendix 2: Storm-water absorption indicators